Journal of Engineering Science and Technology
Vol. 15, No. 3 (2020) 2077 - 2089

INFLUENCE OF ADDITION TIO_2 NANOPARTIELCS ON THE MECHANICAL PROPERTIES OF WELDING JOINTS FOR LOW CARBON STEEL BASE PLATE BY ELECTRIC ARC WELDING

ALI F. AL-OBAIDI[1], ALI S. YASIR[2], S. M. THAHAB[3,4,*]

[1]Southern Cement State Company, Kufa Cement Plant, Najaf. Iraq
[2]Mechanical Engineering Department, Faculty of Engineering, University of Kufa, Najaf, Iraq
[3]Nanotechnology and Advanced Materials Research Unit (NAMRU), Faculty of Engineering, University of Kufa, Najaf, Iraq
[4]Electronics and Communication Department, Faculty of Engineering, University of Kufa, Najaf, Iraq
*Corresponding Author: sabah.alabboodi@uokufa.edu.iq

Abstract

This paper tries to investigate the effects of adding titanium dioxide nanoparticles (TiO_2 NPs) to the welding joints in order to improve the mechanical properties of such welding joints of (St-37) low carbon steel base plate by means of electric arc welding. The cold spray coating method of the TiO_2 NPs is used for the welding joints during the welding process. Three weight fractions of TiO_2 NPs are used (0.75, 1.5, and 2) % respectively. The selected samples from the tensile strength, hardness, and microstructure tests are examined by Scanning Electron Microscope (SEM). The SEM images reveal that there are homogenous regions in the welded joints cross-section in comparison with specimens that contains no TiO_2 NPs addition. Improvements in tensile strength and hardness values of the welded joints with an increase in TiO_2 NPs concentrations are observed. It is found the average value of ultimate tensile strength of the welded sample without TiO_2 NPs is (435.457) MPa, while the average ultimate tensile strength of the welded sample with 2 % TiO_2 NPs is (576.773) MPa with an improvement ratio of (32.45) %. While the result values of Microhardness test for welded samples without and with 2 % TiO_2 NPs are (215.53 and 256.9) HV respectively with an improvement ratio of (27.4) %.

Keywords: Arc welding, Hardness, Nano-welding, Tensile strength, TiO_2 nanoparticles.

1. Introduction

E6013 wire electrodes were utilized in many fields, including welding of the kiln shell for the cement plants and the welding of the mechanical parts for the petrochemical, oil and gas industries [1-3]. The tensile strength and hardness of welded metals and weld joints are effective in their design and application. Throw studies have been conducted in the last years to improve tensile strength, and hardness of low-carbon steel and the welding joints for it [4, 5]. It has been shown that tensile strength can be improved by an aggregate of the enhanced amount of acicular ferrite, the decreased rate of the columnar zone, and the grain improvement. Also, it has been shown that hardness can be improved by increase in the number of nucleation positions on grain size [6].

Moreover, studying the microstructure of welding area structures has presented many types of ferrite, acicular ferrite, of which grain boundary allotriomorphic ferrite, Widmanstätten ferrite and polygonal ferrite. Continuous with various thicknesses of grain boundary layers can present (show) an allotriomorphic ferrite that grows from columnar austenite grain boundaries [7]. Additionally, the Widmanstätten ferrite nucleates could grow from austenite grain boundaries grain boundary or allotriomorphic ferrite layers which form with austenite grains as a thin wedge-shaped laths. At certain range temperature and transformation mechanism, it was observed that the nucleation between acicular ferrite and bainite could be occurring. Forming sheaves of parallel laths presented from the bundle morphology of bainite grow within small austenite grains or austenite grain boundaries. In addition, a fine interlocking microstructure of nucleates intragranular of acicular ferrite could be shaped as a form of separate laths of non-metallic inclusions within large austenite grains [8].

The Increasing in the density of high-angle boundaries resulting from intragranular acicular ferrite lead to prefer and good mixture of strength and impact toughness of weld metals. The change in crack growth direction which presented the Boundaries that act as hard barriers due to the change in crystallographic orientation [5, 9, 10]. In the last twenty years, many researchers have analysed the forming and presenting of intragranular ferrite in weld metals and low alloy steels as well as the influence of non-metallic inclusions in their surface morphology. It was observed that the chemical composition, distribution of inclusions, size and shape of could affect the nucleation sites that formed strongly by intragranular ferrite [11-15].

The TiO_2 Ceramic materials such as TiO_2 [16, 17], TiO [4, 14], and Ti_2O_3 [1, 12, 15] present a strong nucleation in intragranular ferrite in weld metals and low carbon steel. As a result of improving the retarded and nucleation, an increasing in the amount of ferrite could be achieved by the addition TiO_2 NPs in low carbon steel. The microstructure could improve by coating the wire electrodes using nanotechnology with a nanoparticle that improved the microstructure, mechanical properties, and operational behaviour. As an example, a several studies, conducting the using of fine inclusion of the-oxide mixing in austenite grains as coated materials on the wire electrodes [16].

The current study scrutinizes and investigates the effect of TiO_2 NPs on the mechanical properties, the nucleation of intragranular ferrite and microstructure of weld metals by employing the flux design wire electrode [18]. As well as, the current work will present and find an easy way to optimize the mechanical

properties of weld joint such as: tensile strength, hardness, reduction of weld defects, minimizing of grain size in the microstructure, and the stability of microstructural formation.

Also, using TiO_2 NPs as injected colloidal in the welding area instead of using wire welding coat could improve the penetration of nanoparticles inside steel materials and increase the adhesion of nanoparticles within welding area surface. However, using the TiO_2 NPs as injected colloidal could prevent losing large amount of materials if its selected as powder or a wire coat material.

2. Experimental work

Three weight ratio (wt. %) of TiO_2 NPs colloidal (0.75, 1.5, and 2) % was added respectively to weld metal by cold spray coating method which is provided from (US Research. Inc.) as a anatase type with an average particle size of (10-25) nm. The wire electrode AWS E6013 (4mm diameter) has been used to weld specimens. St-37 base metal was used in this research with a dimension of (250 mm x 200 mm x 20 mm). The chemical analysis of wire electrode and base metal was presented in Table 1.

The type of instrument which was used for chemical analysis test is a spectrometer provided from (ARL-3460 Swiss origin).

Table 1. Chemical analysis test (wt. %) of core wire electrode (E6013) and base metal (St-37).

Sample	C	Si	Mn	P	S	Cu	Cr	Ni	Mo	V
Base material	≤ 0.13	0.1-0.4	0.2-0.5	0.05	0.035	0.03 - 0.05	0.05 - 0.08	0.00	0.0	0.0
Wire electrode	0.2	1.0	1.2	N.S	N.S	0.00	0.2	0.3	0.3	0.08

The TiO_2 NPs colloidal was prepared by dissolving the (2.76, 5.52 and 7.36) g TiO_2 NPs in 20 ml of distilled water according to Eq. (1) which was used to prepare weight ratio of (0.75, 1.5 and 2) wt. % of the TiO_2 NPs respectively. These TiO_2 NPs weight ratio samples of welding filler marked as (S_1, S_2, and S_3) samples respectively, as shown in Table 2. Then these samples were stirred using a magnetic stirrer instrument provided from (Jenway Company, UK), and then sonicated using uultrasonic mixing liquid instrument provided from (MTI Corporation company, USA) [19].

$$\boldsymbol{v}\,\% = \frac{\frac{\boldsymbol{w_n}}{\boldsymbol{\rho_n}}}{\frac{\boldsymbol{w_n}}{\boldsymbol{\rho_n}} + \frac{\boldsymbol{w_w}}{\boldsymbol{\rho_w}}} \times \mathbf{100} \quad (1)$$

Table 2. Volume concentrations of TiO_2 NPs with corresponding weight

Specimen	Volume concentration (% wt.)	Weight of TiO_2 nanoparticles (W_n)
S_1	3.41	2.76 g
S_2	6.60	5.52 g
S_3	8.62	7.36 g

The selected weight ratios of the TiO_2 NPs (2.76, 5.52 and 7.36) g was computed by means of calculated the weight ratio between the weight of the welding area and the weight of the added nanoparticles as illustrated in Eq. (2) below:

$$wt\ \% = \frac{w_n}{w_f} \times 100 \quad (2)$$

The cold spray coating method has been applied to the TiO_2 NPs colloidal to each pass of welding process. The welding zone was coated by TiO_2 nanoparticle after cleaning the welding slag and measuring temperature of the welding zone prior to coating process. It was found experimentally that the best adhesives temperature of TiO_2 NPs are obtained at 300 ^{0}C and followed by another welding layer. It is clear that the temperature of the welding zone before the coating is an important factor. Additionally, at high temperatures greater than 500 ^{0}C gets rapid drying in TiO_2 nanoparticle colloidal occurred leading to a situation of flaking and non-adhesion of TiO_2 NPs on the welding zone.

In contrast to that, at low temperatures less than 200 ^{0}C, the colloidal dries slowly so that the colloidal pushed out of the welding zone, because of the pressure of the air compressor. And the temperature value was measured using a manual infrared thermometer instrument. The St-37 specimens have been lathing in mechanical workshop of the Kufa cement plant. The specimens have been welded by using the E6013 (4 mm) wire electrode diameter at 200 A current by AC welding machine, and then the welding is tested by portable ultrasonic flaw detector instrument (USM 35X, Krautkramer Company, Germany origin), to detect the defects of welding before the test, no defects were found in the welding areas.

The limitation of adding the TiO_2 NPs ratio presented at the value of TiO_2 NPs larger than 2% (2.5 %). An increases in spray number of the colloidal on the welding join leads to increase in the thickness of the TiO_2 NPs in the welding area which its causing a breakage in the coating layer and minimizing the attachment to the welding join as shown in Fig. 1.

Fig. 1. Cold spray coating method (TiO_2 >2 %).

2.1. Tensile test

A 20-mm thickness of base plate (St-37) low carbon steel has been used and prepared by cutting the specimens to size of (190 mm x 125 mm) as required for round tensile

specimen is fifteen. Three specimens from base metal (B), three of which are welded without the addition of nanoparticles (W) and the remaining nine from welded with (0.75, 1.5, 2) %, TiO_2 NPs (S_1, S_2, and S_3) respectively. By taken three specimens for each percentage. The weld dimensions of the weld pool of the preparation and formation of the round tensile specimen are shown in Fig. 2.

Since the plate that is used for the designing and preparing of specimens is 20 mm thickness, thus the number of passes to fill the entire welding pool are fourteen passes distributed over seven layers (two pass for each layer). According to our research procedure the TiO_2 NPs are distributed only into four middle layers because they included the diameter of the tensile specimen type and according to the method of addition nanoparticle mentioned above.

Therefore, there is no need to add nanoparticles to the welding layers at the top and bottom of the welding zone. After the welding pool wad fully filled the welding zone of the base metal was cut by an automatic horizontal band saw with coolant solution. The milling machine was used to make the specimen in a regular parallel shape. The lathe machine was used to prepare the weld specimen as shown in Fig. 3.

All operations have been carried out in the mechanical workshop the at Kufa Cement Plant. The type of instrument that used was provided form (BESMAK, 500 KN, Germany origin) at Engineering consulting office at the Faculty of Engineering at the University of Kufa.

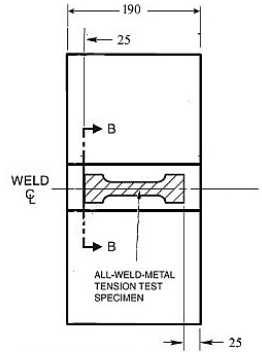

(a) Test plate showing location of test specimen.

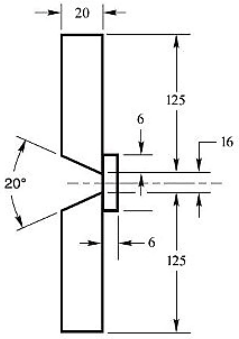

(b) Joint preparation.

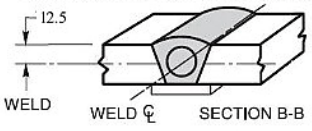

(c) Location of all-weld-metal Tension test specimen.

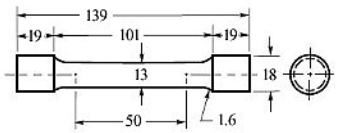

(d) Tension specimen.

Fig. 2. Standard method of round tensile test specimen [20].

Fig. 3. Round tensile specimens as prepared.

2.2. Microhardness test

The Microhardness test was performed for the weld zone. It was cut by hand saw which is taken from round tensile specimens. The specimen dimensions are (Ø 13x10 mm) as shown in Fig. 4. Five specimens were selected as base metal (B), welding without the addition of nanoparticles (W) and other three selected from welding with the addition of a TiO_2 NPs in percentages (0.75, 1.5, 2) % as (S_1, S_2, and S_3) specimens respectively. All the manufacturing processes were done in mechanical workshop of the Kufa Cement Plant/IRAQ.

After preparing the specimens, the specimen surfaces are prepared by grinding and polishing instrument. Grinding paper (silicon carbide) is used in water solution with a grit grade in (240, 320, 400, and 600). Each specimen was grinned for three minutes for each grinding paper. Also, a five specimens were examined by the digital Microhardness test instrument (Type MHV-2000S) of TIME Group Company, China origin) in the laboratory of the materials department at the Faculty of Engineering, University of Kufa, using (9.8 N) load. Three-point test were examined for each specimen and calculated average value for each.

2.3. SEM Microstructure and EDS Tests

In this test, five specimens were cut by hand saw which are taken from round tensile specimens after testing. Followed by choosing one specimen of the base metal (B) and one specimen from welding without the addition of nanoparticles (W). Three specimens welding with the addition of (0.75, 1.5 and 2) % TiO_2 NPs as S_1, S_2, and S_3 were chosen respectively.

The specimen dimensions were selected as (Ø 13x10 mm) as shown in Fig. 4. After the cutting process, the specimen surfaces were prepared, ground and polished by the grinding and polishing instrument. The grades of grinding papers of (240, 320, 400, 600, 800, 1000 and 1200) were chosen respectively. The time of the grinding surface of the specimen are five minutes for each paper grinding. Then the specimen's surfaces were polished using alumina emulsion materials for five minutes in each specimen. The surface of the specimen was etched with 2% Nitric acid (Nital) in Ethanol, by immersing the surface of the specimen for one minute inside the solution. Followed by washing the surface with distilled water and drying in hot dry air. The type of instrument of SEM Microstructure and EDS tests which was used in this research provided from (TESCAN, Mira 3, French origin).

Fig. 4. Prepared specimens for SEM microstructure and EDS tests of (W, S_1, S_2, and S_3) specimens.

3. Results and discussions

Figure 5 shows the ultimate tensile strength results of welded specimens of each concentrations of TiO_2 NPs colloidal. It is observed that the increases in the average tensile strength reached to 576.773 MPa for welding specimens (S_3) as compared to welded specimens (W) which was reached to value of 435.457 MPa.

The maximum improvement in tensile strength value is 32.45% for (S_3) specimen as indicated in the Table 3 and shown in Fig. 6 which is tested using Tensile instrument from (BESMAK, 500 KN, Germany origin with a maximum error class of ± 0.5 %. The increases in the tensile strength related to the aggregated and enhancement of the amount of acicular ferrite. In addition, the decreases rate of the columnar zone and the improvement in the grain size play great role in such behaviour [18, 21].

Table 3. Round tensile test results in (MPa).

Specimens	B	W	S_1	S_2	S_3
1	420.89	438.47	489.7	560.82	575.74
2	416.31	431.69	524.89	551.18	587.95
3	414.54	436.21	520.59	565.95	566.63
AV.	417.24	435.457	511.727	559.317	576.773
Improvement %	0.0	0.0	17.51	28.44	32.45

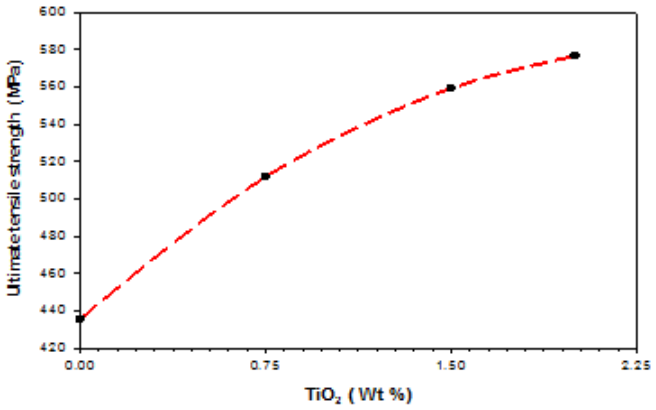

Fig. 5. Ultimate tensile strength as a function of TiO_2 NPs wt. %.

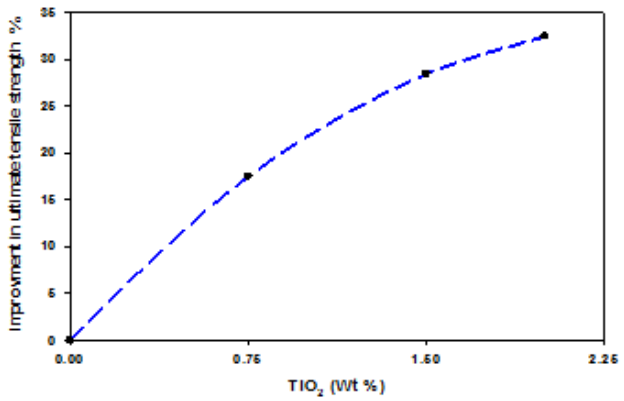

Fig. 6. The improvement percentage in ultimate tensile strength as a function of TiO_2 NP wt. % of (W, S_1, S_2, and S_3) specimens.

Figure 7 shows the Microhardness results of welded specimens of each concentration of TiO_2 NPs colloidal. It is observed that the increasing in the average Microhardness reach to 274.6 J for welding specimens (S_3) as compared to welded specimens (W) which reached to 215.53 J. The maximum improvement value in Microhardness is (27.4 %) for (S_3) specimen as indicated in Table 4 and Fig. 8. The type of instrument employed for this test is (MHV-2000S Digital Micro Hardness Tester, TIME Group Company, China origin, maximum error class of ± 0.5 %. The increases in Microhardness related to the rising in the numbers of nucleation positions on TiO_2 NPs which increases the bonding strength between the grains and leading to an improvement in Microhardness [21].

Table 4. Microhardness test results in (HV) of the specimens.

Specimens	B	W	S_1	S_2	S_3
1	131.43	212.1	271.1	261.1	277.2
2	132.87	223.3	237.2	242.3	281.3
3	128.32	211.2	252.3	267.3	265.3
AV.	130.87	215.53	253.53	256.9	274.6
Improvement %	0.0	0.0	17.63	19.19	27.40

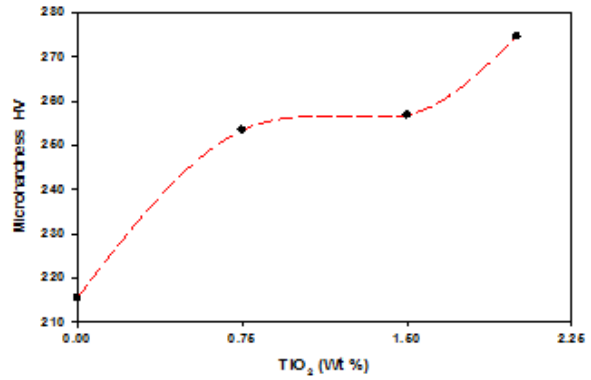

Fig. 7. Microhardness results as a function of TiO_2 NPs wt % for (W, S_1, S_2, and S_3) specimens.

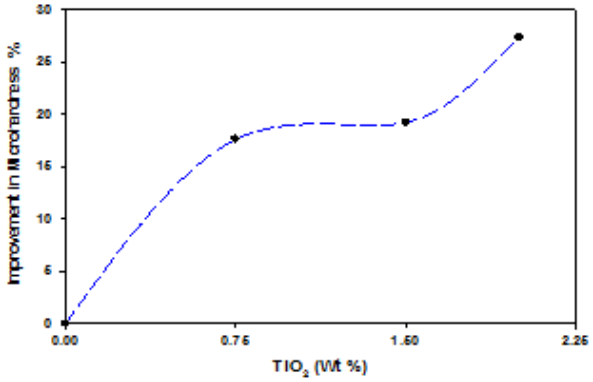

Fig. 8. The improvement percentage in Microhardness results as a function of TiO_2 NPswith % of (W, S_1, S_2, and S_3) specimens.

Figures 9(a) to (d) show the SEM images of cross sections of welded specimens with and without adding TiO_2 NPs. SEM images indicated that there are heterogeneous regions in the microstructure of the welded area for welded specimens without adding TiO_2 NPs as compare to the homogenous regions presented in the specimens welded with adding 2% wt TiO_2 NPs.

In addition, it is found that the increases in the contents of TiO2 NPs led to conversion of columnar zones from Widmanstätten ferrite and allotriomorphic ferrite to fine intragranular ferrite. Thus an enhancement occurs in the ferrite grain size of the weld zone as shown in Fig. 9 in which its leading to an improvement in tensile strength and Microhardness.

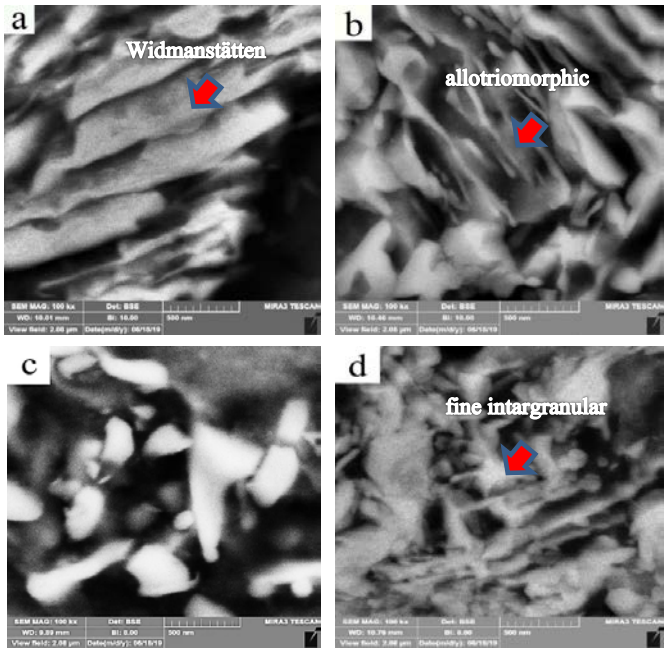

Fig. 9. SEM images (M. 500 nm) of welded specimens (a) W, (b, c, d) for (S_1, S_2, and S_3) specimens respectively.

The results of EDS test reveal that the amount of Ti and Oxygen increased with the addition of TiO_2 NPs to the welding zone. On the contrary, the amount of Mn and Si decreased with the increases of TiO_2 NPs. These results can be described by the following reactions 1, 2 below [19].

$$Si + 2O \leftrightarrow SiO_2 \quad (1)$$

$$SiO_2 + 2Mn \leftrightarrow 2MnO + Si \quad (2)$$

Table 5 reveals the values of the Ti, Oxygen, Mn, Si contains were (1.09, 4.84 9.93 and 3.51 %) respectively for the welding specimen without TiO_2 NPs as shown in Fig. 10.

Table 5. Quantitative results testof the (W) welding specimen.

Elt	Line	Int	Error	K	Kr	wt %
C	Ka	68.5	142.1840	0.0155	0.0138	5.24
O	Ka	133.1	142.1840	0.0306	0.0272	4.84
Si	Ka	103.0	228.8563	0.0256	0.0227	3.51
Ti	La	44.0	144.3423	0.0101	0.0082	1.09
Mn	La	426.5	142.1840	0.0989	0.0878	9.93
Fe	Ka	2572.9	2.9738	0.8186	0.7273	75.39
				1.0000	0.8884	100.00

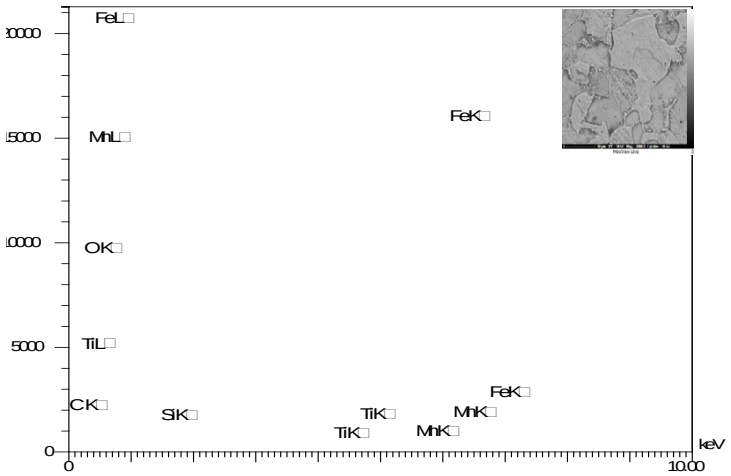

Fig. 10. EDS analysis for the (W) welding specimen.

Table 6 reveals the values of the Ti, Oxygen, Mn, Si contains are (1.27,11.86, 8.56 and 3.06) % respectively for the welding specimen with 2 % TiO_2 NPs as shown in Fig. 11.

Table 6. Quantitative test results of S_3 welding specimen.

Elt	Line	Int	Error	K	Kr	wt %
C	Ka	115.4	144.3423	0.0263	0.0213	7.84
O	Ka	343.6	144.3423	0.0794	0.0643	11.86
Si	Ka	82.1	205.3090	0.0290	0.0234	3.06
Ti	La	49.6	143.8454	0.0113	0.0096	1.27
Mn	La	326.7	144.3423	0.0761	0.0616	8.56
Fe	Ka	2437.4	2.9474	0.7791	0.6305	67.41
				1.0000	0.8093	100.00

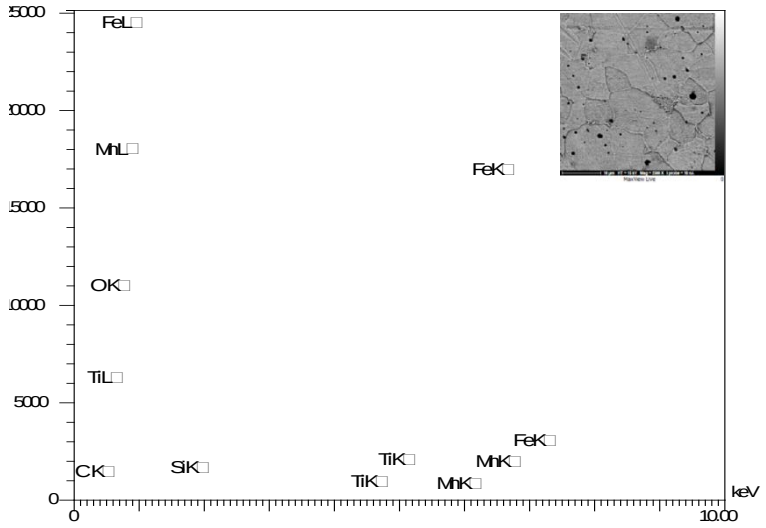

Fig. 11. EDS Analysis for the (S_3) welding specimen.

4. Conclusions

- On the basic of investigating and testing the effect of adding of the TiO_2 NPs colloidal to the welding joints that are welded by wire electrode E6013 in arc welding method. As well as, the tensile strength, Microhardness and microstructure of samples had been studied. Over all outcomes could be concluded as below:
- The addition of TiO_2 NPs colloidal to the welding joints, shows an increase in tensile strength of welding zone because of an aggregate and enhanced the amount of acicular ferrites and the decreasing in the rate of the columnar zone and grain improvement had been presented.
- An increase in Microhardness with the addition of TiO_2 NPs colloidal to the welding joints has been observed in the welding zone due to the increasing in the number of nucleation positions on TiO_2 NPs.
- Adding the TiO_2 NPs colloidal to the welding joints rivals an increases in Ti contains and a decrease in Mn, Si contains, that led to an increase in the amount of acicular ferrite.
- The microstructure of the weld area with the addition of 2 % TiO_2 NPs demonstrated mainly acicular ferrite contents with a small proportion of grain boundary ferrite and very small of Widmanstätten ferrite due to the high TiO_2 NPs contents in the weld zone.
- It had been found that the increases in the contents of TiO_2 NPs led to conversion of columnar zones from Widmanstätten ferrite and allotriomorphic ferrite to fine intragranular ferrite and an enhancement in the ferrite grain size of reheated zones had been presented.
- Based on the aforementioned conclusions the following recommendations could be suggested: Firstly, the effect of adding TiO_2 NPs to wire electrode coating (Type E6013) could be studied. Secondly, the effect of adding TiO_2 NPs as a colloidal to welding area that welding by E7018 wire electrode needs for more

investigation. Third, the effect of adding TiO_2 NPs as a colloidal to welding area on HAZ of welding has to be pondered.

Acknowledgements

The authors would like to acknowledge the assistance offered by Nanotechnology and Advanced Materials Research Unit (NAMRU) and Laboratories of Mechanical Engineering Department at Faculty of Engineering University of Kufa /IRAQ. Also, assists offered by the staff in the mechanical workshop in Kufa cement plant/IRAQ are highly appreciated for their support.

Nomenclatures

v %	Volume concentration
w_f	Weight for welding filler (368 g).
w_n	Weight for nanoparticles (2.76, 5.52 and 7.36) g.
wt. %	Weight ratio (0.75, 1.5, and 2) %.
w_w	Weight for distilled water, g

Greek Symbols

ρ_n	Density for nanoparticles (3.9 g/cm3 for TiO_2 (anatase)).
ρ_w	Density for distilled water (1 g/cm3).

Abbreviations

AC	Alternating Current
AWS	American Welding Society
EDS	Energy Dispersive Spectroscopy
NPs	Nanoparticles
SEM	Scanning Electron Microscope

References

1. Byun, J.S.; Shim, J.H.; Suh, J.Y.; Oh, Y. J.; Cho, Y. W.; Shim, J. D.; and Lee, D.N. (2001). Inoculated acicular ferrite microstructure and mechanical properties. *Materials Science and Engineering*, A, 319, 326-331.
2. Wang, C.; Wang, M.; Shi, J.; Hui, W.; and Dong, H. (2008). Effect of microstructural refinement on the toughness of low carbon martensitic steel. *Scripta Materialia*, 58(6), 492-495.
3. Calcagnotto, M.; Ponge, D.; and Raabe, D. (2010). Effect of grain refinement to 1 μm on strength and toughness of dual-phase steels. *Materials Science and Engineering*, A, 527(29-30), 7832-7840.
4. Pan, T.; Yang, Z.G.; Zhang, C.; Bai, B.Z.; and Fang, H.S. (2006). Kinetics and mechanisms of intragranular ferrite nucleation on non-metallic inclusions in low carbon steels. *Materials Science and Engineering*, A, 438, 1128-1132.
5. Terashima, S.; and Bhadeshia, H.K. (2006). Size distribution of oxides and toughness of steel weld metals. *Science and technology of welding and joining*, 11(5), 580-582.

6. Bose-Filho, W.W.; Carvalho, A.L.; and Strangwood, M. (2007). Effects of alloying elements on the microstructure and inclusion formation in HSLA multipass welds. *Materials Characterization*, 58(1), 29-39.
7. Bhadeshia, H.K. (2001). *Bainite in steals* (2nd ed.). London: The Institute of Materials.
8. Babu, S.S. (2004). The mechanism of acicular ferrite in weld deposits. *Current Opinion in Solid State and Materials Science*, 8(3-4), 267-278.
9. Gourgues A.F.; Flower, H.M.; and Lindley, T.C. (2000). Electron backscattering diffraction study of acicular ferrite, bainite, and martensite steel microstructures. *Materials Science and Technology*, 16(1), 26-40.
10. Diaz-Fuentes, M.; Iza-Mendia, A.; and Gutierrez, I. (2003). Analysis of different acicular ferrite microstructures in low-carbon steels by electron backscattered diffraction. Study of their toughness behaviour. *Metallurgical and Materials Transactions*, A, 34(11), 2505-2516.
11. Wu, K.M. (2006). Three-dimensional analysis of acicular ferrite in a low-carbon steel containing titanium. *Scripta materialia*, 54(4), 569-574.
12. Byun, J.S.; Shim, J.H.; and Cho, Y.W. (2003). Influence of Mn on microstructural evolution in Ti-killed C-Mn steel. *Scripta materialia*, 48(4), 449-454.
13. Shim, J.H.; Oh, Y.J.; Suh, J.Y.; Cho, Y.W.; Shim, J.D.; Byun, J.S.; and Lee, D.N. (2001). Ferrite nucleation potency of non-metallic inclusions in medium carbon steels. *Acta Materialia*, 49(12), 2115-2122.
14. Zhang, D.; Terasaki, H.; and Komizo, Y.I. (2010). In situ observation of the formation of intragranular acicular ferrite at non-metallic inclusions in C-Mn steel. *Acta materialia*, 58(4), 1369-1378.
15. Peng, Y.; Chen, W.; and Xu, Z. (2001). Study of high toughness ferrite wire for submerged arc welding of pipeline steel. *Materials characterization*, 47(1), 67-73.
16. Nedjad, S.H.; and Farzaneh, A. (2007). Formation of fine intragranular ferrite in cast plain carbon steel inoculated by titanium oxide nanopowder. *Scripta Materialia*, 57(10), 937-940.
17. Kiviö, M.; Holappa, L.; and Iung, T. (2010). Addition of dispersoid titanium oxide inclusions in steel and their influence on grain refinement. *Metallurgical and Materials Transactions*, B, 41(6), 1194-1204.
18. Fattahi, M.; Nabhani, N.; Vaezi, M.R.; and Rahimi, E. (2011). Improvement of impact toughness of AWS E6010 weld metal by adding TiO_2 nanoparticles to the electrode coating. *Materials Science and Engineering*, A, 528(27), 8031-8039.
19. https://www.academia.edu/4225801/PREPARATION_AND_ESTIMATION_OF_NANOFLUID By por chelvan
20. AWS B 4.0. (2007), *Standard Methods for Mechanical Testing of Welds* (7th ed.). American Welding Society.
21. Nedjad, S.H.; Moghaddam, Y.Z.; Vazirabadi, A.M.; Shirazi, H.; and Ahmadabadi, M. N. (2011). Grain refinement by cold deformation and recrystallization of bainite and acicular ferrite structures of C-Mn steels. *Materials Science and Engineering*, A, 528(3), 1521-1526.